

Evolution characteristics of central black hole of magnetized accretion disc

D. X. Wang*, K. Xiao, W. H. Lei

Department of Physics, Huazhong University of Science and Technology, Wuhan, 430074, China

**Send offprint requests to: D. X. Wang (dawang@hust.edu.cn)*

Accepted 2002 May 2. Received 2002 April 15; in original form 2002 January 7

ABSTRACT

Evolution characteristics of a Kerr black hole (BH) are investigated by considering coexistence of disc accretion with the Blandford-Znajek process (the BZ process) and magnetic coupling of the BH with the surrounding disc (MC process). (i) The rate of extracting energy from the rotating BH in the BZ process and that in MC process are expressed by a unified formula, which is derived by using an improved equivalent circuit. (ii) The mapping relation between the angular coordinate on the BH horizon and the radial coordinate on the disc is given in the context of general relativity and conservation of magnetic flux. (iii) The power and torque in the BZ process are compared with those in MC process in detail. (iv) Evolution characteristics of the BH and energy extracting efficiency are discussed by using the characteristics functions of BH evolution in the corresponding parameter space. (v) Power dissipation on the BH horizon and BH entropy increase are discussed by considering the coexistence of the above energy mechanisms.

Key words: Accretion, accretion discs – Black hole physics

1 INTRODUCTION

It is well known that magnetized accretion disc of black hole (BH) is an effective model in astrophysics. The interaction between a Kerr BH and the surrounding magnetic field has been used not only to explain high energy radiation and jet production from quasars and active galactic nuclei, but also as a possible central engine for gamma-ray bursts (Rees 1984; Frank, King & Raine 1992; Lee, Wijers & Brown 2000, hereafter LWB). Confined by the magnetic field in the inner region of the disc, the magnetic field lines frozen previously in the disc plasma will deposit on the horizon in company with the accretion onto the BH, and the magnetized disc becomes a good environment for supporting the magnetic field on the horizon. Blandford and Znajek (1977) proposed firstly that the rotating energy and the angular momentum of a BH can be extracted by the surrounding magnetic field, and this energy mechanism has been referred to as the BZ process, in which the BH horizon and the remote astrophysical load are connected by the open magnetic field lines, and energy and angular momentum are extracted from the rotating BH and transported to the remote load.

There still remain some open problems on the BZ process, and one of them is how to estimate the ratio of the angular velocity of the magnetic field lines to that of the BH horizon. Macdonald and Thorne (1982 hereafter MT82) argued in a speculative way that the ratio will be regu-

lated to about 0.5 by the BZ process itself, which corresponds to the optimal value of the extracting power with the impedance matching. However, as argued by Punsly and Coroniti (1990), it is hard to understand how the load can conspire with the BH to have the same resistance and satisfy the matching condition, since the load is so far from the BH that it cannot be casually connected.

Recently some authors (Blandford 1999; Li 2000a, 2000b; Li & Paczynski 2000) argued that with the existence of the closed field lines a fast rotating BH will exert a torque on the disc to transfer energy and angular momentum from the BH to the disc. Henceforth this energy mechanism is referred to as magnetic coupling (MC) process. Compared with the BZ process, the load in MC process is the surrounding disc, which is much better understood than the remote load though the magnetohydrodynamics (MHD) of the disc is still very complicated.

Some works have been done to discuss the influence of the BZ process on the evolution of BH accretion disc (Park & Vishniac 1988; Moderski & Sikora 1996; Lu et al. 1996; Wang et al. 1998, hereafter WLY). However MC effects involving the closed field lines were not taken into account in the previous works. In fact the closed field lines should exist on the horizon as well as the open field lines, and disc accretion should coexist with the BZ and MC process. In this paper evolution characteristics of a Kerr BH are investigated by considering coexistence of disc accretion with the

BZ and MC process (henceforce DABZMC).

In order to facilitate the discussion of the evolution of the central BH surrounded by the magnetized accretion disc we make the following assumptions:

(i) The disc is perfectly conducting and the magnetic field lines are frozen in the disc. The magnetosphere is stationary, axisymmetric and force-free outside the BH and the disc (MT82);

(ii) The magnetic field is so weak that its influence on the dynamics of the particles in the disc is negligible, and the BH has an external geometry of Kerr metric;

(iii) The disc is thin and Keplerian, lies in the equatorial plane of the BH with the inner boundary being at the marginally stable orbit.

This paper is organized as follows. In Sec.II the rate of extracting energy from the rotating BH in the BZ process (henceforce the BZ power) and that in MC process (henceforce MC power) are expressed by a unified formula, which is derived by using an improved equivalent circuit based on MT82. Our result for the BZ power is consistent with that derived in LWB. In Sec.III a mapping relation between the angular coordinate on the BH horizon and the radial coordinate on the disc is given in the context of general relativity and conservation of magnetic flux. In Sec.IV The power and torque in the BZ process are compared with those in MC process in detail. In Sec.V evolution characteristics of the BH and energy extracting efficiency are discussed by using the characteristics functions in the corresponding parameter space. In Sec.VI we discuss the power dissipation on the BH horizon and the BH entropy increase, and show that the excess rate of change of BH entropy does come from the total power dissipation on the BH horizon in the BZ and MC process. Finally, in Sec.VII, we summarize our main results.

2 DERIVATION OF BZ POWER AND MC POWER

Two mechanisms of magnetic extraction of energy from a rotating BH are involved in our model, i.e., the BZ process and MC process. The configuration of the poloidal magnetic field of the BH magnetosphere for the coexistence of DABZMC is shown in Fig.1, where the angular coordinate of the open field lines is assumed to vary from 0 to θ_M , and that of the closed field lines from θ_M to $\pi/2$. θ_M is a parameter indicating the angular boundary between the open and the closed field lines, and the BZ and MC effects vanish as $\theta_M = 0$ and $\theta_M = \pi/2$, respectively.

Considering that both mechanisms arise from the rotation of the Kerr BH relative to the surrounding magnetic field, we expect that the BZ power and MC power can be expressed by a unified formula. In order to do this we proposed a model, in which the remote load in the BZ process and the load disc in MC process are incorporated into a unified load with resistance Z_L and angular velocity Ω_L . Based on MT82 an improved equivalent circuit is shown in Fig.2, in which a series of loops correspond to the adjacent magnetic surfaces consisting of the field lines connecting the BH horizon and the load.

In the i -loop of Fig.2 segments PS (characterized by the flux Ψ) and QR (characterized by the flux $\Psi + \Delta\Psi$) represent two adjacent magnetic surfaces, and segments PQ and

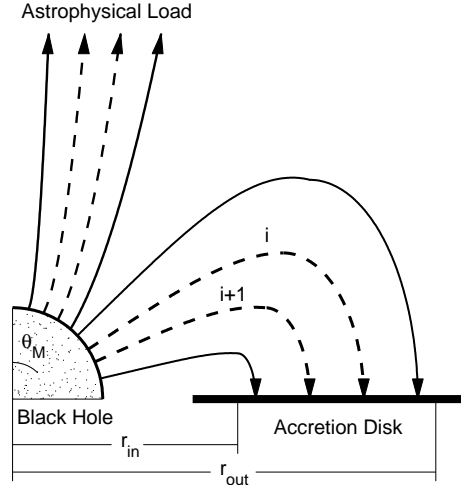


Figure 1. The configuration of the poloidal magnetic field of the BH magnetosphere.

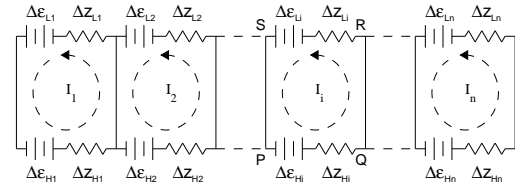


Figure 2. An improved equivalent circuit for a unified model for the BZ and MC process.

RS represent the BH horizon and the load sandwiched by the two surfaces. ΔZ_H and ΔZ_L (hereafter subscript "i" is omitted) are the corresponding resistances of the BH horizon and the load, respectively. $\Delta\epsilon_H = (\Delta\Psi/2\pi)\Omega_H$ and $\Delta\epsilon_L = -(\Delta\Psi/2\pi)\Omega_L$ are electromotive forces due to the rotation of the BH and the load, respectively. The minus sign in the expression of $\Delta\epsilon_L$ arises from the direction of the flux. Ω_H in the expression of $\Delta\epsilon_H$ is the angular velocity of the BH horizon and reads ($G=c=1$):

$$\Omega_H = a_*/(2r_H), r_H = M(1+q), q = \sqrt{1-a_*^2} \quad (1)$$

where a_* is the BH spin, which is related to BH mass M and angular momentum J by $a_* \equiv J/M^2$, and r_H is the radius of the BH horizon. By using the BH magnetosphere model given in MT82 we obtain the following equations:

$$\int_P^Q \alpha \vec{E} \cdot d\vec{l} = \Delta V_H = (\Delta\Psi/2\pi)(\omega_H - \Omega_F) = (\Delta\Psi/2\pi)(\Omega_H - \Omega_F) = I\Delta Z_H \quad (2)$$

$$\int_R^S \alpha (\vec{E} + \vec{v}_L \times \vec{B}) \cdot d\vec{l} = \Delta V_L + (\Delta\Psi/2\pi)(\omega_L - \Omega_L) = (\Delta\Psi/2\pi)(\Omega_F - \Omega_L) = I\Delta Z_L \quad (3)$$

$$\Delta V_L = \int_R^S \alpha \vec{E} \cdot d\vec{l} = (\Delta\Psi/2\pi)(\Omega_F - \omega_L) \quad (4)$$

where ΔV_H and ΔV_L are the potential drops measured by "zero-angular-momentum observers" (ZAMOs) on the BH horizon and on the load, respectively. ZAMOs is a family of fiducial observers defined by Bardeen et al (1972). \vec{v}_L is the load's velocity relative to ZAMOs. ω_H ($\rightarrow \Omega_H$) and ω_L are the ZAMO angular velocities on the BH horizon and the

load, respectively. Ω_F is the angular velocity of the magnetic field lines. $\alpha \equiv (d\tau/dt)_{Z_{AMO}}$ is the "lapse function", which is written as follows:

$$\alpha = \rho\sqrt{\Delta}/\Sigma \quad (5)$$

where Σ , ρ and Δ are the Kerr metric parameters and read

$$\begin{aligned} \Sigma^2 &\equiv (r^2 + a^2)^2 - a^2 \Delta \sin^2 \theta, \rho^2 \equiv r^2 + a^2 \cos^2 \theta \\ \Delta &\equiv r^2 + a^2 - 2Mr \end{aligned} \quad (6)$$

Incorporating equations (2) and (3) we obtain

$$\begin{aligned} \Delta\varepsilon_H + \Delta\varepsilon_L &= \int_P^Q \alpha \vec{E} \cdot d\vec{l} + \int_R^S \alpha (\vec{E} + \vec{v}_L \times \vec{B}) \cdot d\vec{l} \\ &= I(\Delta Z_H + \Delta Z_L) \end{aligned} \quad (7)$$

Dividing equation (2) by equation (3), we derive the relation relating the three angular velocities, Ω_H , Ω_L and Ω_F as follows:

$$\Omega_F = (\Omega_H \Delta Z_L + \Omega_L \Delta Z_H) / (\Delta Z_H + \Delta Z_L) \quad (8)$$

Assuming $\Omega_L = 0$ in the BZ process, we have

$$\Omega_F = \Omega_H \Delta Z_L / (\Delta Z_H + \Delta Z_L) \quad (9)$$

Considering that the load disc consists of plasma of perfect conductivity and the magnetic field lines are frozen in the disc plasma, we have $\Delta Z_L = 0$ and

$$\Omega_F = \Omega_L = \Omega_D = \frac{1}{M(\chi^3 + a_*)} \quad (10)$$

where Ω_D is the angular velocity of the disc at the place where the magnetic flux penetrates, and $\chi = \sqrt{r/M}$ is dimensionless radial coordinate of the disc. The current I in each loop can be expressed by

$$\begin{aligned} I &= \frac{\Delta\varepsilon_H + \Delta\varepsilon_L}{\Delta Z_H + \Delta Z_L} = (\Delta\Psi/2\pi) \frac{\Omega_H - \Omega_L}{\Delta Z_H + \Delta Z_L} \\ &= (\Delta\Psi/2\pi) \frac{\Omega_H - \Omega_F}{\Delta Z_H} \end{aligned} \quad (11)$$

where equation (8) is used in deriving the right-hand side (RHS) of equation (11). The current I on the BH horizon feels Ampere's force, and the torque exerted on the annular ring of the width $\Delta l = \rho \Delta \theta$ is

$$\Delta T = \varpi B_H I \Delta l = (\Delta\Psi/2\pi)^2 (\Omega_H - \Omega_F) / \Delta Z_H \quad (12)$$

where $\Delta\Psi = B_H 2\pi \varpi \Delta l$, B_H is the magnetic field on the horizon, and $\varpi = (\Sigma/\rho) \sin \theta$ is the cylindrical radius of the horizon. Therefore the extracting power between the two adjacent magnetic surfaces is

$$\Delta P = \Omega_F \Delta T = (\Delta\Psi/2\pi)^2 \Omega_F (\Omega_H - \Omega_F) / \Delta Z_H \quad (13)$$

where

$$\Delta Z_H = R_H \Delta l / (2\pi \varpi) = 2\rho \Delta \theta / \varpi \quad (14)$$

and $R_H = 4\pi/c = 377 \text{ohm}$ is the surface resistivity of the BH horizon. Considering that the BH horizon consists of two hemispheres and integrating equations (13) and (12) over the angular coordinate from $\theta = 0$ to θ_M we obtain the total BZ power and torque as follows:

$$P_{BZ}/P_0 = 2a_*^2 \int_0^{\theta_M} \frac{k(1-k)\sin^3 \theta d\theta}{2 - (1-q)\sin^2 \theta} \quad (15)$$

$$T_{BZ}/T_0 = 4a_*(1+q) \int_0^{\theta_M} \frac{(1-k)\sin^3 \theta d\theta}{2 - (1-q)\sin^2 \theta} \quad (16)$$

where $k \equiv \Omega_F/\Omega_H$ and

$$\begin{cases} P_0 = \langle B_H^2 \rangle M^2 \approx B_4^2 M_8^2 \times 6.59 \times 10^{44} \text{erg} \cdot \text{s}^{-1} \\ T_0 = \langle B_H^2 \rangle M^3 \approx B_4^2 M_8^3 \times 3.26 \times 10^{47} \text{g} \cdot \text{cm}^2 \cdot \text{s}^{-2} \end{cases} \quad (17)$$

In equation (17) $\langle B_H^2 \rangle$ is the average value of B_H^2 over the BH horizon, B_4 and M_8 are $\sqrt{\langle B_H^2 \rangle}$ and M in the units of 10^4gauss and $10^8 M_\odot$, respectively. Hereafter $\langle B_H^2 \rangle$ is regarded as a constant on the horizon, and the sign of the average value is omitted. Taking $\theta_M = \pi/2$ and $k = 0.5$ in equation (15) we obtain the optimal BZ power as follows:

$$\begin{aligned} P_{BZ}^{optimal}/P_0 &= Q^{-1} (\arctan Q - a_*/2), \\ Q &\equiv \sqrt{(1-q)/(1+q)} \end{aligned} \quad (18)$$

This result is exactly the same as derived by Lee et al, who pointed out that the BZ power had been underestimated by a factor ten in previous work (LWB). The corresponding optimal BZ torque can be expressed by

$$T_{BZ}^{optimal}/P_0 = 4Q^{-2} (\arctan Q - a_*/2) \quad (19)$$

Similarly, taking $\Omega_F = \Omega_D$ and integrating equations (13) and (12) over the angular coordinate from θ_M to $\pi/2$, we obtain total MC power and torque as follow:

$$P_{MC}/P_0 = 2a_*^2 \int_{\theta_M}^{\pi/2} \frac{\beta(1-\beta)\sin^3 \theta d\theta}{2 - (1-q)\sin^2 \theta} \quad (20)$$

$$T_{MC}/T_0 = 4a_*(1+q) \int_{\theta_M}^{\pi/2} \frac{(1-\beta)\sin^3 \theta d\theta}{2 - (1-q)\sin^2 \theta} \quad (21)$$

where

$$\beta \equiv \Omega_D/\Omega_H = \frac{2(1+q)}{a_*(\chi^3 + a_*)} \quad (22)$$

Inspecting equations (15), (16), (20) and (21), we find the expressions for P_{BZ} and T_{BZ} are almost the same as those for P_{MC} and T_{MC} except that k is replaced by β . From equation (9) we know that the parameter $k \equiv \Omega_F/\Omega_H$ is uncertain due to lack of the knowledge about "the remote astrophysical load", while β can be determined by equation (22) as a function of a_* and χ .

3 MAPPING RELATION BETWEEN BH HORIZON AND MC REGION OF DISC

In order to calculate P_{MC} and T_{MC} we should first determine the mapping relation between the BH horizon and the disc. Considering the flux tube consisting of two adjacent magnetic surfaces "i" and "i+1" as shown in Fig.1, we have $\Delta\Psi_H = \Delta\Psi_D$ required by continuum of magnetic flux, i.e.,

$$B_H 2\pi (\varpi \rho)_{r=r_H} d\theta = -B_D 2\pi (\varpi \rho / \sqrt{\Delta})_{\theta=\pi/2} dr \quad (23)$$

where B_D is the poloidal component of the magnetic field on the disc and

$$(\varpi \rho)_{r=r_H} = (\Sigma \sin \theta)_{r=r_H} = 2Mr_H \sin \theta \quad (24)$$

$$(\varpi \rho / \sqrt{\Delta})_{\theta=\pi/2} = \Sigma / \sqrt{\Delta} = \alpha^{-1} \rho \quad (25)$$

where

$$\alpha = (\rho\sqrt{\Delta}/\Sigma)_{\theta=\pi/2} = \sqrt{\frac{1 - 2\chi_{ms}^{-2}\xi^{-1} + a_*^2\chi_{ms}^{-4}\xi^{-2}}{1 + a_*^2\chi_{ms}^{-4}\xi^{-2} + 2a_*^2\chi_{ms}^{-6}\xi^{-3}}} \quad (26)$$

Following Blandford (1976) we assume that B_D varies as

$$B_D \propto \xi^{-n} \quad (27)$$

where $\xi \equiv r/r_{ms}$ is a dimensionless radial parameter defined in terms of the radius r_{ms} of the marginally stable orbit (Bardeen et al 1972).

Assuming that the inner boundary of the MC region is located at the inner edge of the disc, and considering the balance of the magnetic pressures between the horizon and the inner edge of the disc (Ghosh & Abramowicz 1997), we assume

$$B_H = B_D|_{\xi=1} \quad (28)$$

Incorporating equations (27) and (28) we have

$$B_D = B_H \xi^{-n} \quad (29)$$

Substituting equations (24), (25) and (29) into equation (23) we have

$$\sin \theta d\theta = -G(a_*, \xi, n) d\xi \quad (30)$$

where

$$G(a_*, \xi, n) = \frac{\chi_{ms}^4 \xi^{-n+1}}{2(1+q)} \sqrt{\frac{1 + a_*^2 \chi_{ms}^{-4} \xi^{-2} + 2a_*^2 \chi_{ms}^{-6} \xi^{-3}}{1 - 2\chi_{ms}^{-2} \xi^{-1} + a_*^2 \chi_{ms}^{-4} \xi^{-2}}} \quad (31)$$

Integrating equation (30) we have

$$\cos \theta_M - \cos \theta = - \int_{\xi_{out}}^{\xi} G(a_*, \xi, n) d\xi \quad (32)$$

Setting $\xi = \xi_{in} = 1$ at $\theta = \pi/2$, we have

$$\cos \theta_M = \int_1^{\xi_{out}} G(a_*, \xi, n) d\xi \quad (33)$$

Thus the mapping relation between the angular coordinate on the horizon and the radial coordinate on the disc is derived in the context of general relativity and conservation of magnetic flux as follows:

$$\cos \theta = \int_1^{\xi} G(a_*, \xi, n) d\xi \quad (34)$$

It is noted that equation (33) provides a constraint to the outer boundary of the MC region, which is represented by $\xi_{out} \equiv r_{out}/r_{ms}$, provided that the parameters a_* , θ_M and n are given. ξ_{out} turns out to be a function of n , varying monotonically for the given a_* and θ_M as shown in Fig.3, and it behaves as a function of a_* varying non-monotonically for the given n and θ_M as shown in Fig.4. Since ξ_{out} is limited, the parameter n should be less than one critical value n_c corresponding to infinite ξ_{out} . The curves of n_c versus a_* for the given values of θ_M are shown in Fig.5.

4 COMPARISON OF POWER AND TORQUE IN THE BZ PROCESS AND MC PROCESS

In order to compare the relative strength of MC power to the BZ power and torque we define the ratio of P_{MC} to $P_{BZ}^{optimal}$

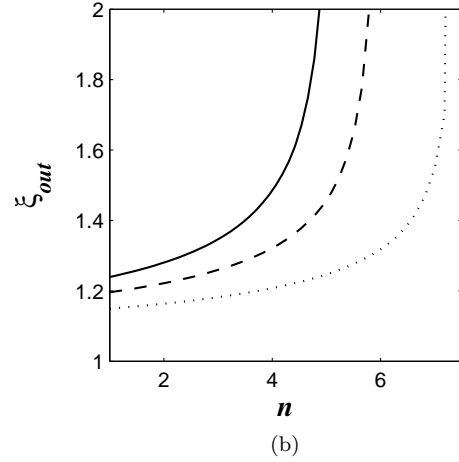
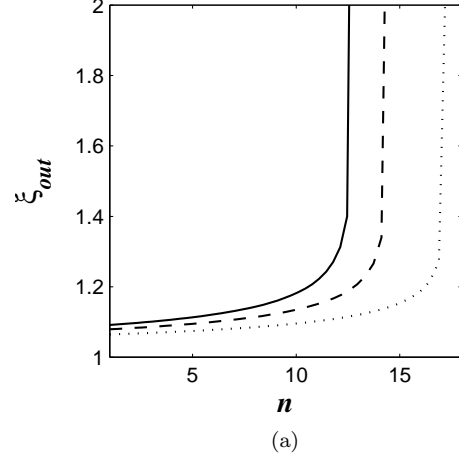


Figure 3. The curves of ξ_{out} versus n for the given values of θ_M with $\theta_M = 0$ (solid line), $\pi/6$ (dashed line) and $\pi/4$ (dotted line); (a) $a_* = 0$, (b) $a_* = 0.998$.

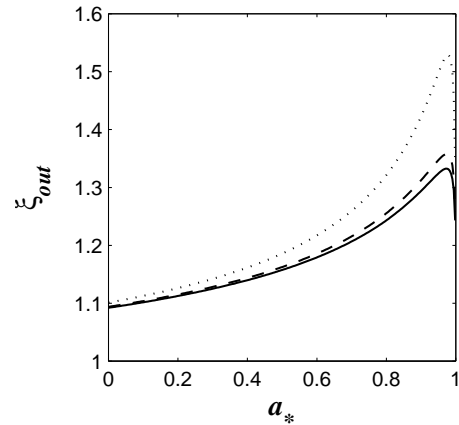


Figure 4. The curves of ξ_{out} versus a_* for $\theta_M = 0$ and $0 < a_* < 0.998$ with $n = 1.1$ (solid line), $n = 1.5$ (dashed line), and $n = 3$ (dotted line).

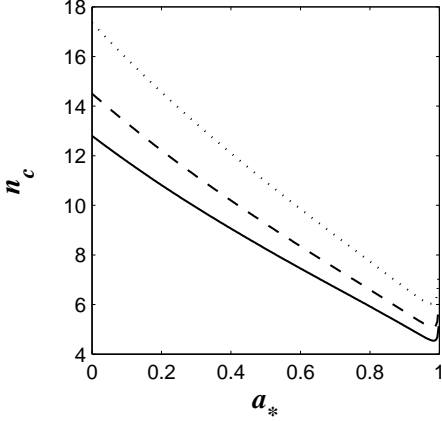


Figure 5. The curves of n_c versus a_* for the given values of θ_M with $\theta_M = 0$ (solid line), $\pi/6$ (dashed line) and $\pi/4$ (dotted line).

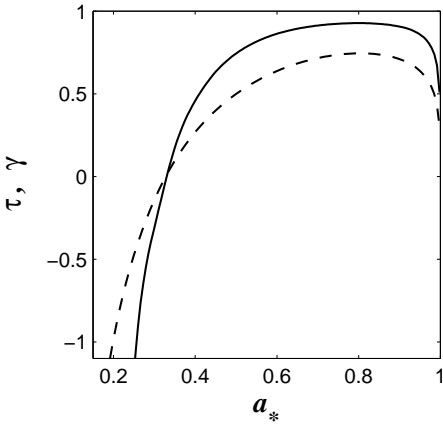


Figure 6. The curves of γ (solid line) and τ (dashed line) versus the BH spin a_* for $n = 1.1$ and $0.2 < a_* < 0.998$.

and that of T_{MC} to $T_{BZ}^{optimal}$ as follows,

$$\begin{aligned} \gamma &\equiv P_{MC}/P_{BZ}^{optimal} \\ &= \frac{2a_*^2 Q}{(\arctan Q - a_*/2)} \int_{\theta_M}^{\pi/2} \frac{\beta(1-\beta)\sin^3\theta d\theta}{2-(1-q)\sin^2\theta} \end{aligned} \quad (35)$$

$$\begin{aligned} \tau &\equiv T_{MC}/T_{BZ}^{optimal} \\ &= \frac{a_*^2 Q}{(\arctan Q - a_*/2)} \int_{\theta_M}^{\pi/2} \frac{(1-\beta)\sin^3\theta d\theta}{2-(1-q)\sin^2\theta} \end{aligned} \quad (36)$$

Setting $\theta_M = 0$ in equations (35) and (36), we have the curves of γ and τ versus a_* for the given parameter n , and those versus n for the given a_* as shown in Fig.6 and Fig.7, respectively.

The values of a_* corresponding to the three special values of γ ($\gamma = -1, 0$ and γ_{max}) and to those of τ ($\tau = -1, 0$ and τ_{max}) are calculated for the given values of n as shown in Table 1 and Table 2, respectively.

From the above calculations on γ and τ we obtain the following results:

(i) The signs of P_{MC} and T_{MC} are the same as the corresponding γ and τ , and they change from the negative to the positive at $a_*^{\gamma^2}$ and $a_*^{\tau^2}$ respectively. It is shown in Table

Table 1. The three special values of γ and the values of the concerning parameters

n	$\gamma = -1$	$\gamma = 0$	$\gamma = \gamma_{max}$
1.1	$a_*^{\gamma^1} = 0.2583$	$a_*^{\gamma^2} = 0.3286$	$a_*^{\gamma^m} = 0.7997,$ $\gamma_{max} = 0.9278$
1.5	$a_*^{\gamma^1} = 0.2581$	$a_*^{\gamma^2} = 0.3283$	$a_*^{\gamma^m} = 0.8002,$ $\gamma_{max} = 0.9287$
3.0	$a_*^{\gamma^1} = 0.2572$	$a_*^{\gamma^2} = 0.3269$	$a_*^{\gamma^m} = 0.8021,$ $\gamma_{max} = 0.9325$

Table 2. The three special values of τ and the values of the concerning parameters

n	$\tau = -1$	$\tau = 0$	$\tau = \tau_{max}$
1.1	$a_*^{\tau^1} = 0.1988$	$a_*^{\tau^2} = 0.3278$	$a_*^{\tau^m} = 0.8045,$ $\tau_{max} = 0.7452$
1.5	$a_*^{\tau^1} = 0.1987$	$a_*^{\tau^2} = 0.3275$	$a_*^{\tau^m} = 0.8056,$ $\tau_{max} = 0.7481$
3.0	$a_*^{\tau^1} = 0.1980$	$a_*^{\tau^2} = 0.3260$	$a_*^{\tau^m} = 0.8118,$ $\tau_{max} = 0.7614$

1 and Table 2 that $a_*^{\tau^2}$ is a little less than $a_*^{\gamma^2}$. Therefore both energy and angular momentum are transferred from the BH to the disc as $a_* > a_*^{\gamma^2}$, and transferred from the disc to the BH as $a_* < a_*^{\tau^2}$. It is interesting to notice that the transfer direction of energy is opposite to that of angular momentum for $a_*^{\tau^2} < a_* < a_*^{\gamma^2}$, i.e., energy is transferred from the disc to the BH, while angular momentum from the BH to the disc in this value range of the BH spin.

(ii) Both γ and τ vary non-monotonically as a_* for the given parameter n , and attain their maxima at $a_*^{\gamma^m}$ and $a_*^{\tau^m}$, respectively;

(iii) The maxima of P_{MC} and T_{MC} are all less than the corresponding $P_{BZ}^{optimal}$ and $T_{BZ}^{optimal}$, respectively, while the absolute values of the former two are greater than the corresponding values of the latter two as a_* is less than $a_*^{\gamma^1}$ and $a_*^{\tau^1}$, respectively.

(iv) As shown in Fig.7, both γ and τ increase very little as the increasing parameter n , which implies that both P_{MC}

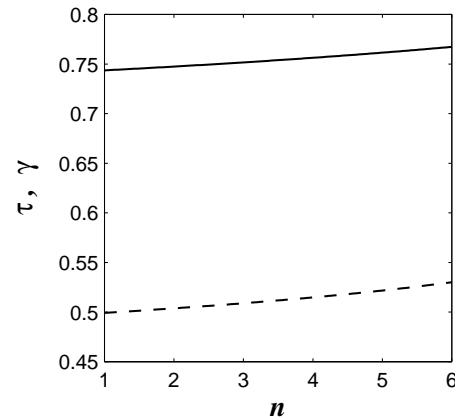


Figure 7. The curves of γ (solid line) and τ (dashed line) versus the power-law index n for $a_* = 0.5$ and $1 < n < 6$.

and T_{MC} are insensitive to the power-law index n of the radial coordinate ξ .

5 EVOLUTION CHARACTERISTICS AND ENERGY EXTRACTING EFFICIENCY

Based on conservation of energy and angular momentum the basic evolution equations of the Kerr BH in the coexistence of DABZMC are written as follows:

$$dM/dt = E_{ms}\dot{M}_D - P_{BZ} - P_{MC} \quad (37)$$

$$dJ/dt = L_{ms}\dot{M}_D - T_{BZ} - T_{MC} \quad (38)$$

Incorporating equations (37) and (38), we have the evolution equation for the BH spin as follows:

$$da_*/dt = M^{-2} (L_{ms}\dot{M}_D - T_{BZ} - T_{MC}) - 2M^{-1}a_* (E_{ms}\dot{M}_D - P_{BZ} - P_{MC}) \quad (39)$$

where \dot{M}_D is the accretion rate of rest mass, E_{ms} and L_{ms} are specific energy and specific angular momentum corresponding to the inner edge radius r_{ms} , respectively.

Since the magnetic field on the BH is supported by the surrounding disc, there are some relations between B_H and \dot{M}_D . As a matter of fact these relations might be rather complicated, and would be very different in different situations. One of them is given to investigate the correlation between BH spin and dichotomy of quasars by considering the balance between the pressure of the magnetic field on the horizon and the ram pressure of the innermost parts of an accretion flow (Moderski, Sikora & Lasota 1997), i.e.,

$$B_H^2/(8\pi) = P_{ram} \sim \rho c^2 \sim \dot{M}_D/(4\pi r_H^2) \quad (40)$$

From equation (40) we assume the relation as

$$\dot{M}_D = B_H^2 M^2 (1+q)^2/2 \quad (41)$$

However equation (41) is derived without MC effects. By considering the transfer of the energy and angular momentum between the BH and the disc equations (41) is modified as follows:

$$\dot{M}_D = B_H^2 M^2 (1+q)^2/2 + [1 - \delta(\theta_M - \pi/2)] (\dot{M}_D)_{mc} \quad (42)$$

where $(\dot{M}_D)_{mc}$ is the MC correction to the accretion rate at the inner edge of the disc, and it reads

$$(\dot{M}_D)_{mc} = -\frac{4B_H^2 M^2 Q (\chi_{ms}^3 + a_*)^2 (1-\beta)}{(\chi_{ms}^3 + 4a_*)} \sqrt{\frac{1+a_*^2 \chi_{ms}^{-4} + 2a_*^2 \chi_{ms}^{-6}}{1-2\chi_{ms}^{-2} + a_*^2 \chi_{ms}^{-4}}} \quad (43)$$

The derivation of equation (43) is given in Appendix A. To exclude $(\dot{M}_D)_{mc}$ from the case without magnetic coupling we define $\delta(\theta_M - \pi/2)$ as follows:

$$\delta(\theta_M - \pi/2) \equiv \begin{cases} 1, & \theta_M = \pi/2, \\ 0, & 0 \leq \theta_M < \pi/2 \end{cases} \quad (44)$$

Thus the equation (42) is applicable to the coexistence of DABZMC.

Setting $\dot{M}_D = 0$ in equation (42), we can derive a value of the BH spin, $a_*^{stop} \approx 0.4677$, at which the accretion will stop at the inner edge of the disc. Substituting equation (42) into equations (37)–(39), we have

$$dM/dt = f(a_*, u_j) \dot{M}_D \quad (45)$$

$$dJ/dt = Mh(a_*, u_j) \dot{M}_D \quad (46)$$

$$da_*/dt = M^{-1}g(a_*, u_j) \dot{M}_D \quad (47)$$

where

$$g(a_*, u_j) = h(a_*, u_j) - 2a_* f(a_*, u_j) \quad (48)$$

In the above equations $u_j \equiv \theta_M, k, n$ is used for simplicity to represent the three parameters other than a_* . $f(a_*, u_j)$ and $g(a_*, u_j)$ are referred to as the characteristics functions (CFs) of BH evolution.

5.1 Evolution characteristics of Kerr BH

First we discuss the evolution characteristics of the Kerr BH in the coexistence of disc accretion with the BZ process for $\theta_M = \pi/2$. From equations (37)–(39) we have the CFs as follows:

$$f(a_*, k) = E_{ms} - P_{BZ}/\dot{M}_D \quad (49)$$

$$h(a_*, k) = M^{-1} (L_{ms} - T_{BZ}/\dot{M}_D) \quad (50)$$

$$g(a_*, k) = h(a_*, k) - 2a_* f(a_*, k) \quad (51)$$

From equations (45) and (47) we find that the signs of dM/dt and da_*/dt are the same as those of $f(a_*, k)$ and $g(a_*, k)$, respectively. As shown in Fig.8 we have the curve represented by $g(a_*, k) = 0$ in the 2-dimension space consisting of the parameters a_* and k , which divides the parameter space into two regions. And each black dot with arrowhead is referred to as a representative point (RP), which represents one BH evolution state. We can use RP's displacement in the parameter space to describe BH evolution visually. According to the positions of RPs we have two evolution modes of the BH, and the details are given as follows.

(I) Region I: $f(a_*, k) > 0$ and $g(a_*, k) < 0$.

Mode I: RPs in Region I always move towards the left until they arrive at the boundary curve $g(a_*, k) = 0$, i.e., BH will reach its equilibrium spin a_*^{eq} in long enough evolution time. RPs in region I represent the BHs with increasing mass and decreasing spin.

(II) Region II: $f(a_*, k) > 0$ and $g(a_*, k) > 0$.

Mode II: RPs in Region II always move towards the right until they arrive at the boundary curve $g(a_*, k) = 0$, i.e., BH will reach its equilibrium spin a_*^{eq} in long enough evolution time. RPs in region II represent the BHs with increasing mass and increasing spin.

Next we shall discuss BH evolution in the coexistence of disc accretion with MC process. Substituting $\theta_M = 0$ and equation (42) into equations (37)–(39), we have the corresponding CFs as follows:

$$f(a_*, n) = E_{ms} - P_{MC}/\dot{M}_D \quad (52)$$

$$h(a_*, n) = M^{-1} (L_{ms} - T_{MC}/\dot{M}_D) \quad (53)$$

$$g(a_*, n) = h(a_*, n) - 2a_* f(a_*, n) \quad (54)$$

We can also describe BH evolution by using the displacement of RPs in 2-dimension parameter space consisting of the parameters a_* and n as shown in Fig.9, which is divided

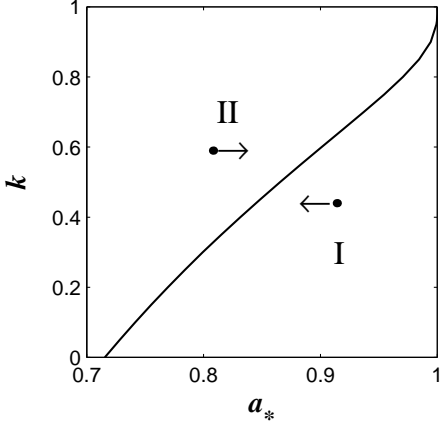


Figure 8. Parameter space for BH evolution in the BZ process with $0 < k < 1$ and $0.7 < a_* < 1$.

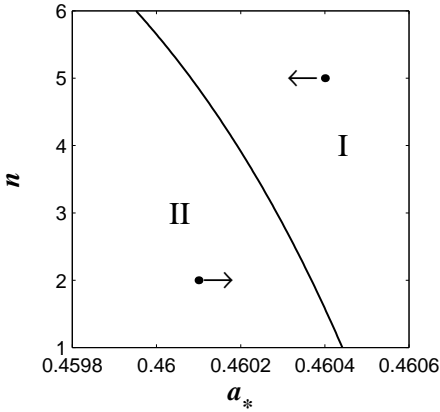


Figure 9. Parameter space for BH evolution in MC process with $1 < n < 6$ and $0.4598 < a_* < 0.4606$.

into two regions by the curve $g(a_*, n) = 0$. In this case the description of the BH evolution characteristics and the two evolution modes are almost the same as that given in the BZ process except that $f(a_*, k)$ and $g(a_*, k)$ are replaced by $f(a_*, n)$ and $g(a_*, n)$, respectively. Inspecting Fig.8 and Fig.9, we have the following results:

(i) The CFs in the corresponding parameter space can be used to describe the evolution characteristics of the BH in a visual way. If we know the initial position of RP in the parameter space, we can determine the evolution characteristics of the BH immediately.

(ii) The effects of the parameter k and n on the BH evolution in the BZ and MC process can be easily found in the corresponding parameter space. From Fig.8 we find that a_*^{eq} increases as the increasing k , which is consistent with our previous work (WLY). On the other hand, we find from Fig.9 that a_*^{eq} increases very little as the decreasing n . Our calculations show that the values of a_*^{eq} are very near to and a little less than $a_*^{stop} \approx 0.4677$.

(iii) As shown in Fig.5, the value range of n is limited and confined by conservation of magnetic flux. Compared with the parameter k , the effects of n on the variation of a_*^{eq} are very weak for the confined value range of n .

5.2 Energy extracting efficiency of BH accretion disc

Energy extracting efficiency of BH accretion disc can be investigated also by using the CFs. From equations (45) and (47) we have

$$dM/M = [f(a_*, u_j)/g(a_*, u_j)] da_* \quad (55)$$

As is well known, a Kerr BH can be characterized by its mass M and spin a_* . If a Kerr BH evolves from the initial state (a_{*0}, M_0) to the state (a_*, M) , the BH mass can be expressed by

$$M = M_0 \exp \left[\int_{a_{*0}}^{a_*} \frac{f(a'_*, u_j)}{g(a'_*, u_j)} da'_* \right]. \quad (56)$$

The efficiency corresponding to the evolution process of BH can be defined as

$$\eta_p = \frac{M_D - (M - M_0)}{M_D} = 1 - \frac{M/M_0 - 1}{M_D/M_0} \quad (57)$$

which is the efficiency of converting accreted mass into radiation energy during the evolution process, and M_D is the accreted rest mass and expressed as a function of a_* by using equations (47) and (56) as follows:

$$M_D = M_0 \int_{a_{*0}}^{a_*} \frac{1}{g(a_*, u_j)} \exp \left[\int_{a_{*0}}^{a_*} \frac{f(a'_*, u_j)}{g(a'_*, u_j)} da'_* \right] da_* \quad (58)$$

The efficiency corresponding to each evolving state of the BH is defined as

$$\eta_s = \frac{dM_D - dM}{dM_D} = 1 - (dM/dt)/\dot{M}_D = 1 - f(a_*, u_j) \quad (59)$$

From equation (37) we find that efficiency η_s is equal to the sum of the following three terms:

$$\eta_s = \eta_{DA} + \eta_{BZ} + \eta_{MC} \quad (60)$$

where $\eta_{DA} = 1 - E_{ms}$, $\eta_{BZ} = P_{BZ}/\dot{M}_D$ and $\eta_{MC} = P_{MC}/\dot{M}_D$ are the contributions of disc accretion, the BZ process and MC process, respectively. From equation (47) we know that the equilibrium spin a_*^{eq} is determined by

$$g(a_*, u_j) = 0 \quad (61)$$

Incorporating equations (55)–(59), we have

$$\eta_p|_{a_* \rightarrow a_*^{eq}} = \lim_{a_* \rightarrow a_*^{eq}} (1 - A/B) \quad (62)$$

In equation (62) we have

$$A \equiv \exp \int_{a_{*0}}^{a_*} \frac{f(a'_*, u_j)}{g(a'_*, u_j)} da'_* - 1 \rightarrow \infty$$

and

$$B \equiv \int_{a_{*0}}^{a_*} \frac{1}{g(a_*, u_j)} \exp \left[\int_{a_{*0}}^{a_*} \frac{f(a'_*, u_j)}{g(a'_*, u_j)} da'_* \right] da_* \rightarrow \infty$$

By using L' Hospital limit rule for ∞/∞ type we have

$$\eta_p|_{a_* \rightarrow a_*^{eq}} = 1 - f(a_*^{eq}, u_j) = \eta_s^{eq}(a_*^{eq}, u_j) \quad (63)$$

where η_s^{eq} represents the efficiency η_s at a_*^{eq} . Equation (63) implies that the efficiency η_p is exactly equal to η_s^{eq} , provided

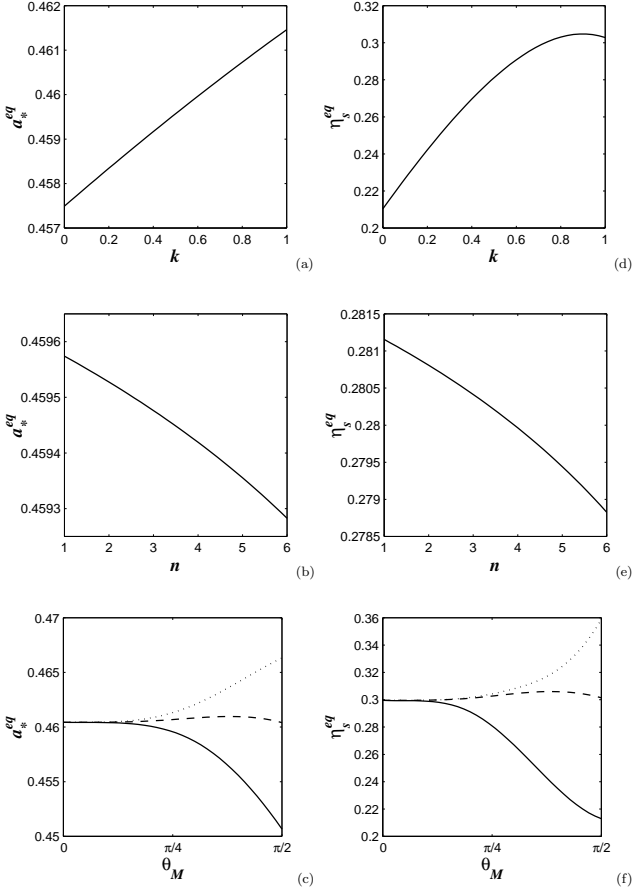


Figure 10. The curves of a_*^{eq} and η_s^{eq} varying as the concerning parameters. (a), (d) $\theta_M = \pi/4$, $0 < k < 1$, $n = 1.1$; (b), (e) $\theta_M = \pi/4$, $k = 0.5$, $1 < n < 6$; (c), (f) $0 < \theta_M < \pi/2$, $n = 1.1$, $k = 0.5$ (solid line), $k = 0.788$ (dashed line); $k = 0.96$ (dotted line).

that a BH evolves from any spin a_{*0} to its equilibrium spin a_*^{eq} . Incorporating equations (42), (59), (61) and (37)–(39), we obtain the curves of a_*^{eq} and η_s^{eq} varying as the concerning parameters are shown in Fig.10.

Comparing Fig.10a, b, c with Fig.10d, e, f we find the following results:

(i) The curves of a_*^{eq} and η_s^{eq} varying as the concerning parameters look very alike except that η_s^{eq} varies as k non-monotonically with its maximum $(\eta_s^{eq})_{max} \approx 30.5\%$ at $a_*^{eq} \approx 0.4611$ for $k \approx 0.8998$ as shown in Fig.10d.

(ii) Both a_*^{eq} and η_s^{eq} decrease monotonically as the increasing n for $\theta_M = \pi/4$ as shown in Fig.10b and Fig.10e. Considering that the outer boundary ξ_{out} increase monotonically as the increasing n , we infer that the more concentrated is the magnetic field on the central region of the disc, the wider is the MC region on the disc, the stronger is the braking effects of MC process on the BH spin, and the lower are the a_*^{eq} and η_s^{eq} .

(iii) As shown in Figs.10c and 10f the variations of a_*^{eq} and η_s^{eq} as θ_M display different characteristics for different values of parameter k : They might increase as θ_M (dotted line) or decreases as θ_M (solid line) or almost remain unchanged with θ_M (dashed line). It is not difficult to understand these results by considering that θ_M is the angular

boundary between the open and closed field lines on the BH horizon: The different variations of a_*^{eq} and η_s^{eq} as θ_M come from the different contributions due to the BZ and MC process. For example, a_*^{eq} and η_s^{eq} will increase as θ_M , if the contributions of the open field lines in unit angular coordinate are greater than those corresponding to the closed ones, while they will decrease as θ_M in case that the former is less than the latter.

In summary we can calculate the efficiency in an evolution process and that corresponding to each evolving state of the Kerr BH by using the equations (57) and (59), respectively, and both of which are expressed in terms of the CFs.

6 BH ENTROPY CHANGE IN COEXISTENCE OF DABZMC

It was shown that the excess rate of change of entropy of the central BH in the BZ process comes from the total power dissipation on the BH horizon (WLY). It is attractive for us to extend this result to the coexistence of DABZMC. As is well known, the BH temperature T_H and entropy S_H can be expressed as (Thorne, Price & Macdonald 1986, hereafter TPM)

$$T_H = \frac{q}{4\pi M(1+q)}, S_H = 2\pi M^2(1+q) \quad (64)$$

Incorporating the basic evolution equations (37), (38) and (39), we have the following equations,

$$T_H dS_H/dt = dM/dt - \Omega_H dJ/dt = (E_{ms} - \Omega_H L_{ms})\dot{M}_D + (\Omega_H T_{BZ} - P_{BZ}) + (\Omega_H T_{MC} - P_{MC}) \quad (65)$$

equation (65) is exactly the mathematical formulation of the first law of thermodynamics for a Kerr BH (TPM). Obviously, the first term on RHS of equation (65) is the contribution due to disc accretion. It is easy to prove that the second and the third term arise from power dissipation on the BH horizon due to the BZ and MC process, respectively. By using the improved equivalent circuit as shown in Fig.2 and equation (11) we have

$$I\Delta\varepsilon_H = I^2\Delta Z_H + I^2\Delta Z_L - I\Delta\varepsilon_L \quad (66)$$

Incorporating equations (9), (11), (13) and $\Delta\varepsilon_L = -(\Delta\Psi/2\pi)\Omega_L$ we obtain

$$\Delta P = (\Delta\Psi/2\pi)^2 \frac{\Omega_F(\Omega_H - \Omega_F)}{\Delta Z_H} = I^2\Delta Z_L - I\Delta\varepsilon_L \quad (67)$$

From equations (66) and (67) we find that $I\Delta\varepsilon_H$ consists of two parts: the extracting power ΔP and the dissipated power ΔP_{DSP} . The extracting power is transferred to the load including both the remote astrophysical load and the load disc. For the BZ process $\Delta\varepsilon_L = 0$, we have

$$\Delta P = \Delta P_{BZ} = I^2\Delta Z_L = (\Delta\Psi/2\pi)^2 \frac{\Omega_F(\Omega_H - \Omega_F)}{\Delta Z_H} \quad (68)$$

For MC process $\Delta Z_L = 0$, we have

$$\Delta P = \Delta P_{MC} = -I\Delta\varepsilon_L = (\Delta\Psi/2\pi)^2 \frac{\Omega_D(\Omega_H - \Omega_D)}{\Delta Z_H} \quad (69)$$

Incorporating equations (11), (12) and (13), we can express the dissipated power ΔP_{DSP} on the BH horizon as

$$\Delta P_{DSP} = I^2\Delta Z_H = (\Delta\Psi/2\pi)^2 (\Omega_H - \Omega_F)^2 / \Delta Z_H$$

$$= \Omega_H \Delta T - \Delta P \quad (70)$$

Integrating equation (70) over the angular coordinate θ , we obtain the total dissipated power on the horizon, which is exactly equal to the sum of the second and the third term on RHS of equation (65), i.e.,

$$P_{DSP} = (P_{DSP})_{BZ} + (P_{DSP})_{MC} \quad (71)$$

where $(P_{DSP})_{BZ} = (\Omega_H T_{BZ} - P_{BZ})$ and $(P_{DSP})_{MC} = (\Omega_H T_{MC} - P_{MC})$ are the total power dissipation due to the BZ and MC process, respectively. Combining equations (15), (16), (20) and (21) we have

$$\begin{aligned} (P_{DSP})_{BZ} &= \Omega_H T_{BZ} - P_{BZ} \\ &= 2a_*^2 B_H^2 M^2 \int_0^{\theta_M} \frac{(1-k)^2 \sin^3 \theta d\theta}{2 - (1-q) \sin^2 \theta} \end{aligned} \quad (72)$$

$$\begin{aligned} (P_{DSP})_{MC} &= \Omega_H T_{MC} - P_{MC} \\ &= 2a_*^2 B_H^2 M^2 \int_{\theta_M}^{\pi/2} \frac{(1-\beta)^2 \sin^3 \theta d\theta}{2 - (1-q) \sin^2 \theta} \end{aligned} \quad (73)$$

Incorporating equations (65), (72) and (73), we express the rates of change of BH entropy corresponding to disc accretion, the BZ and MC process as follows:

$$(dS_H/dt)_{DA} = T_H^{-1} (E_{ms} - \Omega_H L_{ms}) \dot{M}_D \quad (74)$$

$$(dS_H/dt)_{BZ} = T_H^{-1} (\Omega_H T_{BZ} - P_{BZ}) \quad (75)$$

$$(dS_H/dt)_{MC} = T_H^{-1} (\Omega_H T_{MC} - P_{MC}) \quad (76)$$

From the above analysis we conclude that the excess rate of change of the BH entropy does come from the total power dissipation on the BH horizon in the BZ and MC process.

The ratios of the rates of BH entropy change can be written by

$$\begin{aligned} R_{BZDA}(a_*, \theta_M, k) &= \frac{(dS_H/dt)_{BZ}}{(dS_H/dt)_{DA}} \\ &= \frac{\Omega_H T_{BZ} - P_{BZ}}{(E_{ms} - \Omega_H L_{ms}) \dot{M}_D} \end{aligned} \quad (77)$$

$$\begin{aligned} R_{MCDA}(a_*, \theta_M, n) &= \frac{(dS_H/dt)_{MC}}{(dS_H/dt)_{DA}} \\ &= \frac{\Omega_H T_{MC} - P_{MC}}{(E_{ms} - \Omega_H L_{ms}) \dot{M}_D} \end{aligned} \quad (78)$$

where the four parameters k , a_* , θ_M and n are involved. Letting one of them vary and the rest be fixed, we have the curves of R_{BZDA} and R_{MCDA} versus a_* and θ_M as shown in Fig.11, and the following results are obtained:

(i) As shown in Figs.11a and 11b R_{BZDA} increases monotonically as a_* for the given values of k and θ_M , while R_{MCDA} varies non-monotonically and attains a minimum approach zero at $a_* \approx 0.3305$ for the given values of n and θ_M . From the discussion in Sec.IV we know that the minimum of R_{MCDA} arises from the neighboring a_*^2 and $a_*^{\tau^2}$ corresponding to $P_{MC} = 0$ and $T_{MC} = 0$, respectively.

(ii) As shown in Figs.11a and 11b we have $R_{MCDA} > R_{BZDA}$ for $0 < a_* < 0.2694$ and $0.4373 < a_* < a_*^{eq}$, which implies that the contribution to P_{DSP} and BH entropy increase due to MC process dominates over that due to the BZ process in the above value range of the BH spin.

(iii) As shown in Fig.11c the ratio R_{BZDA} increases monotonically as θ_M for the given values of a_* and k , while

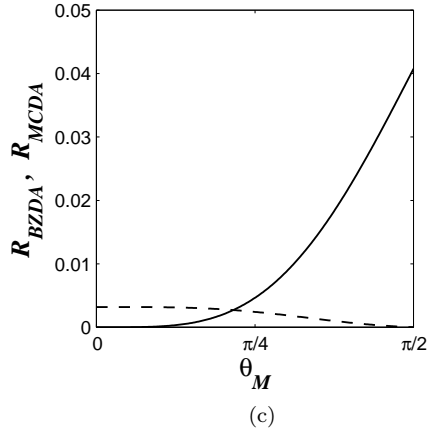
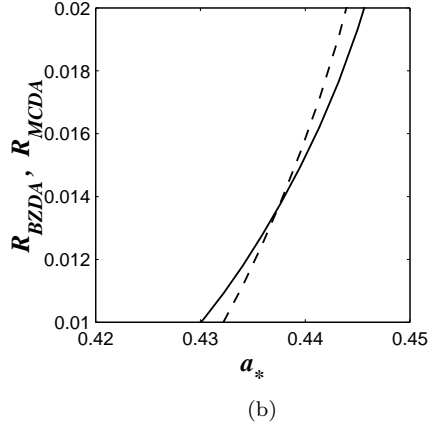
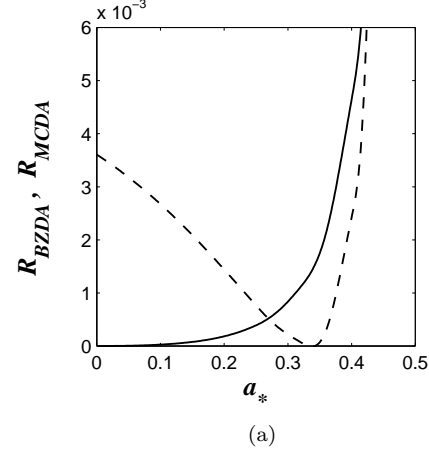


Figure 11. The curves of R_{BZDA} (solid line) and R_{MCDA} (dashed line) versus the concerning parameters, (a), (b) $0 < a_* < 1$, $\theta_M = \pi/4$, $k = 0.5$, $n = 1.1$; (c) $0 < \theta_M < \pi/2$, $a_* = 0.4$, $k = 0.5$, $n = 1.1$.

R_{MCDA} varies non-monotonically as θ_M for the above given values of a_* and n . R_{MCDA} is greater than R_{BZDA} for $0 < \theta_M < 0.6782$, while the former is much less than the latter for $0.6782 < \theta_M < \pi/2$. It is obvious that the sum of the two is much less than unity, which implies that the contribution to BH entropy increase is dominated by disc accretion in the coexistence of DABZMC.

7 SUMMARY

In this paper the evolution characteristics of a Kerr BH and some related issues, such as energy extracting efficiency and entropy change on the BH horizon, are investigated by considering coexistence of DABZMC. By using an improved equivalent circuit a unified expression for the BZ power and MC power are derived. Starting from the conservation laws of energy and angular momentum, we obtain the basic evolution equations of the BH and the CFs in terms of four parameters related to our model, i.e., a_* , θ_M , k and n . We find that the evolution characteristics of the Kerr BH can be well described by using the CHs and the RPs in the corresponding parameter space.

It turns out that the main difference between the BZ process and MC process lies in the two kinds of loads: the remote load with an unknown parameter k for the BZ process, and the load disc with the parameter β for MC process. Parameter k is uncertain, while β is thoroughly determined by the BH spin and the place where the magnetic flux penetrates. The effects of MC process on the evolution of the BH and the efficiency of BH accretion disc can be discussed in virtue of the parameters a_* , θ_M and n , into which the parameter β is merged.

In this model the mapping relation between the BH horizon and the disc is derived by assuming a power-law of the magnetic field varying as the radial coordinate of the disc. It is shown that the power-law index n is related to the outer boundary parameter ξ_{out} . And the MC correction to the accretion rate is considered by using the conservation law of angular momentum. Only the accretion rate at the inner edge of the disc being involved in the evolution equations of the BH, the correction to the accretion rate is made by taking the corresponding values at r_{ms} in our simplified model.

In summary this model provides an analytic approach to the evolution characteristics and related physical quantities of a Kerr black hole surrounded by magnetized accretion disc.

ACKNOWLEDGEMENTS

This work is supported by the National Natural Science Foundation of China under Grant No. 10173004. We are very grateful to the anonymous referee for his suggestions about the MC effects on the accretion rate and the constraints to the parameters of MC process.

APPENDIX A: DERIVATION OF EQUATION(43)

In the case without magnetic coupling between the BH and the disc, accretion is produced by the internal viscous torque T_{vis} of the disc. By using the conservation law of angular momentum the accretion rate \dot{M}_D is related to T_{vis} by the following equation (Frank, King & Raine 1992):

$$-\dot{M}_D \partial(r^2 \Omega_D) / \partial r = \partial T_{vis} / \partial r \quad (A1)$$

where $\partial T_{vis} / \partial r$ is the contribution due to internal viscous torque, always transporting angular momentum outward in

the disc. Taking MC effects into account, we think equation (A1) should be modified by

$$-\dot{M}_D \partial(r^2 \Omega_D) / \partial r = \partial T_{vis} / \partial r - \partial T_{MC} / \partial r \quad (A2)$$

where $\partial T_{MC} / \partial r$ is the contribution due to MC torque, and the minus sign arises from the consideration that the contribution of $\partial T_{vis} / \partial r$ should be counteracted by $\partial T_{MC} / \partial r$ in case $\Omega_D < \Omega_H$. Comparing equations (A1) and (A2), we express $(\dot{M}_D)_{mc}$, the contribution of MC effects to the accretion rate, as follows:

$$(\dot{M}_D)_{mc} = \frac{\partial T_{MC}}{\partial(r^2 \Omega_D)} = \frac{\partial T_{MC} / \partial r}{\partial(r^2 \Omega_D) / \partial r} \quad (A3)$$

Substituting equations (6), (10), (12), (14) and (34) into equation (A3), we have

$$\begin{aligned} (\dot{M}_D)_{mc} &= \frac{4B_H^2 M^3 a_* (1+q)(1-\beta) \sin^2 \theta}{2 - (1-q) \sin^2 \theta} \\ &\times \frac{2(\chi^3 + a_*)^2}{r_{ms} \chi^2 (\chi^3 + 4a_*)} G(a_*; \xi, n) \end{aligned} \quad (A4)$$

From equation (A4) we find that the MC correction depends on the place on the disc where the MC torque acts. Substituting the boundary values such as $\xi = \xi_{in} = 1$ (i.e., $r = r_{ms} = M\chi_{ms}^2$) and $\theta = \pi/2$ into equation (A4) we obtain equation (43), which is the MC correction to the accretion rate at the inner edge of the disc. In derivation the factor 2 is given for the two faces of the disc, and B_H^2 is also taken as the average value over the BH horizon.

REFERENCES

- Bardeen J. M., Press W. H., and Teukolsky S. A., 1972, ApJ, 178, 347
- Blandford R. D., 1976, MNRAS, 176, 465
- Blandford R. D., Znajek R. L., 1977, MNRAS, 179, 433
- Blandford R. D., 1999 in *Astrophysical Discs: An EC Summer School*, Astronomical Society of the Pacific Conference Series, ed. Scullwood J A & Goodman J 160, 265. 1999 preprint astro-ph/9902001
- Frank J., King A. R., Raine D. L., 1985, *Accretion Power in Astrophysics*, Cambridge Univ. Press, Cambridge
- Ghosh P., Abramowicz M. A., 1997, MNRAS 292, 887
- Lee H. K., Wijers R. A. M. J., Brown G. E., 2000, Phys. Rep., 325, 83 (LWB) preprint astro-ph/9906213
- Li L. -X. 2000a, ApJ, 533, 115L.
- Li L. -X. 2000b, preprint astro-ph/0012469
- Li L. -X., Paczynski B., 2000, ApJ, 534, 197L
- Lu Y. J., Zhou Y. Y., Yu K. N., Young, E. C. M., 1996, ApJ, 472, 564
- Macdonald D., Thorne K. S., 1982, MNRAS, 198, 345 (MT82)
- Moderski R., Sikora M., 1996, MNRAS, 283, 854
- Moderski R., Sikora M., Lasota J.P., 1997, in *Relativistic Jets in AGNs* eds.M. Ostrowski, M. Sikora, G. Madejski & M. Belgelman, Krakow 1997, 110, preprint astro-ph/9706263
- Park S. J., Vishniac E. T., 1988, ApJ, 332, 135
- Punsly B., Coroniti F. V., 1990, ApJ, 350, 518
- Rees M. J., 1984, ARA&A. 22, 471
- Shapiro S. L., Teukolsky S. A., 1983, *Black Holes, White Dwarfs and Neutron Stars*, John Wiley & Sons, Inc. New York
- Thorne K. S., Price R. H., Macdonald D. A., 1986, *Black Holes: The Membrane Paradigm*, Yale Univ. Press, New Haven and London (TPM)
- Wang D. X., Lu Y., Yang L. T., 1998, MNRAS, 294, 667 (WLY)